Nanoscale

Accepted Manuscript

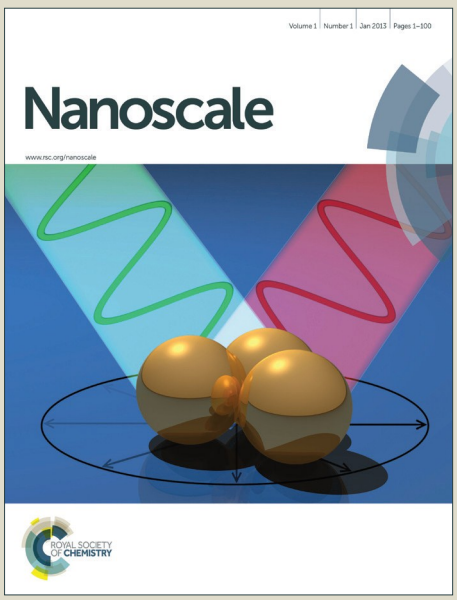

ROYAL SOCIETY OF CHEMISTRY

www.rsc.org/nanoscale

Journal Name

RSCPublishing

ARTICLE

Aptamer-Targeting Photoresponsive Drug Delivery System Using "Off-On" Graphene Oxide Wrapped Mesoporous Silica Nanoparticles

Cite this: DOI: 10.1039/xoxxoooooox

Received ooth January 2012,
Accepted ooth January 2012

DOI: 10.1039/xoxxoooooox

www.rsc.org/

Yuxia Tang, [ab] Hao Hu,[b] Molly Gu Zhang,[b] Jibin Song,[b] Liming Nie,[c] Shouju Wang,[a] Gang Niu,[b] Peng Huang[*b], Guangming Lu[*a], and Xiaoyuan Chen[*b]

We have developed a novel aptamer-targeting photoresponsive drug delivery system by non-covalent assembly of Cy5.5-AS1411 aptamer conjugate on the surface of graphene oxide wrapped doxorubicin (Dox)-loaded mesoporous silica nanoparticles (MSN-Dox@GO-Apt) for light-mediated drug release and aptamer-targeted cancer therapy. The MSN-Dox@GO-Apt with two "off-on" switches were controlled by aptamer targeting and light triggering, respectively. The Cy5.5-AS1411 ligand provides MSN-Dox@GO-Apt with nucleolin specific targeting ability and real-time indicator by "off-on" Cy5.5 fluorescence recovery. The GO acts as a gatekeeper to prevent the loaded Dox from leaking in the absence of laser irradiation, and to control the Dox release in response to laser irradiation. When GO wrapping falls off upon laser irradiation, the "off-on" photoresponsive drug delivery system is activated, thus inducing chemotherapy. Interestingly, with the increase of laser power, the synergism of chemotherapy and photothermal therapy in a single MSN-Dox@GO-Apt platform led to much more effective cancer cell killing than monotherapies, providing a new arsenal against cancer.

Introduction

Photoresponsive drug delivery systems (PDDS) have been developed for intellective drug control release to reduce the side effects of traditional chemotherapy on normal tissues and improve therapeutic efficacy in treating lesions.[1-8] Typically, ultraviolet (UV), visible (Vis) or near-infrared (NIR) lights are used as exogenous stimuli to trigger drug release.[2] However, UV or Vis lights exhibit high toxicity to normal tissue or low penetration depth (~10 mm) due to the strong scattering of skin and soft tissues in this optical window.[2, 4] Therefore, the development of NIR-light triggered PDDS with deeper penetration, lower scattering and minimal harm is highly desirable.[9]

Mesoporous silica nanoparticles (MSNs), due to their large loading capacity, high thermal stability, good biocompatibility, and versatile chemistry for surface functionalization, have been employed as building blocks for PDDS.[10, 11] For MSN-based PDDS, the light-sensitive gatekeepers are utilized to block the pores of the MSNs and prevent guest drugs from leaking. UV-Vis reversible photoisomerization of the azobenzene group (and its derivatives),[12-14] UV spiropyran–merocyanine isomerization,[15] and photodimerization–cleavage cycle of thymine[16] have been reported as intelligent switches for the opening and closing of the pore mouths of MSNs. However, most of these strategies are rather complicated and time-consuming. Meanwhile, the occupation of gatekeepers at important locations of the pore interior or mouth would jeopardize either drug loading or release efficiency.[12] Therefore, it is desirable to find a better way to gatekeep the MSN-based PDDS.

Graphene oxide (GO), a flexible 2-dimensional carbon nanosheet, has been widely used as the basic building block of hierarchical ensembles due to its light and heat sensitivity, as well as good biocompatibility and highly functional surface.[17-19] GO can effectively transduce NIR light into heat, potentially acting as a photothermal switch for controlled drug release. GO also exhibits unique capacities such as DNA/RNA adsorption [20, 21] and excellent quenching ability of dye-labeled DNA/RNA.[22] Wang *et al.*[22] used GO to deliver dye-labeled aptamer to demonstrate that GO can serve as a platform with high fluorescence quenching efficiency for targeted imaging in living cells. Recently, GO has been used to enwrap MSNs, gold nanoparticles and gold nanorods.[23-25] By proper wrapping, GO can act as a great gatekeeper for MSNs without occupying the pore interior or mouth. Zhao *et al.*[23] reported a hybrid material using GO sheets to wrap squaraine dyes loaded MSNs to protect the dye molecules from nucleophilic attack. Therefore, GO can potentially play multi-roles in the construction and development of PDDSs.

Besides intelligent photoactivation, the active targeting function of PDDS is also very important to deliver drugs/agents to specific disease sites or cell populations such as tumor cells. Aptamers, a

class of artificial DNA/RNA probes, have attracted much attention in the engineering of target platforms.[26] They have significant advantages over antibodies, such as flexible design, inexpensive synthesis, easy modification, low immunogenicity and rapid tissue penetration.[20, 26] AS1411, a 26 nt G-rich DNA aptamer, which recognizes nucleolin on the surface of cancer cells with high affinity and specificity, has been widely reported for tumor targeting.[27-29]

Herein we strategically designed and constructed a novel photoresponsive drug delivery system based on graphene oxide wrapped mesoporous silica nanoparticles (MSN@GO) for light-mediated drug release and aptamer-targeted cancer therapy (**Scheme 1**). The model drug, doxorubicin (Dox), was loaded by MSN. Then, negatively-charged GO nanosheets were successfully wrapped around the surface of the positively-charged MSN *via* electrostatic interactions. Afterwards, Cy5.5-labeled AS1411 aptamer (Cy5.5-AS1411) was assembled on the surface of GO *via* hydrophobic interactions and π–π stacking, with dramatic quenching of Cy5.5 fluorescence. After selective uptake of the nanocarrier *via* nucleolin (NCL) receptor-mediated endocytosis, the Cy5.5 fluorescence will be recovered. In the absence of laser irradiation, GO is remarkably stable and efficiently protects the loaded drug from leaking. Upon laser irradiation, GO transduces NIR light into heat and the local high temperature leads to the expansion of GO sheets and vibration of GO and MSNs, causing on-demand Dox release.

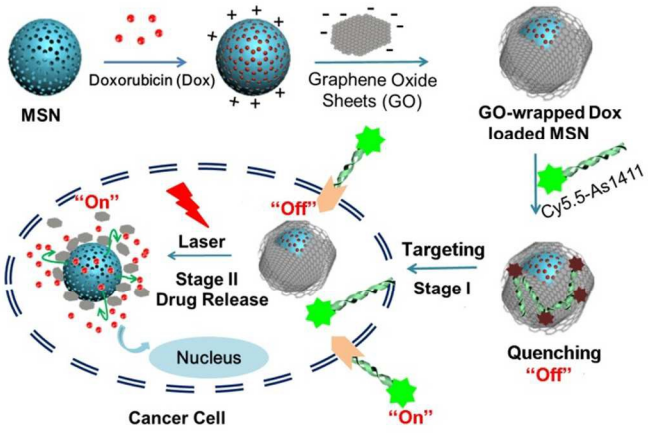

Scheme 1. Schematic illustration of GO-wrapped Dox-loaded MSN-NH_2 bound with Cy5.5-labeled AS1411 aptamer and the corresponding NIR light-controlled intracellular drug release. The MSN-Dox@GO-Apt with two "off-on" switches were controlled by aptamer targeting and light triggering, respectively.

MSNs were synthesized according to a previously reported method.[30, 31] As shown in **Fig. 1a**, MSNs present well-defined spherical nanostructures with radial mesoporous channels. Different sized GO sheets were obtained by the sonication cutting approach. The hydrodynamic size of GO sheets decreased with prolonged sonication time (**Fig. S1**). GO sheets sized 151 ± 11 nm at 2 h sonication were chosen for wrapping experiments. In a typical experiment, Dox was loaded by the MSNs at a pH of 7.4 (MSN-Dox) and the loading efficiency was 17% when 1 mg of MSNs was mixed with 0.5 mg of Dox. MSN-Dox was then mixed with GO under gentle sonication for a few minutes and stirred for 24 h to obtain GO wrapped MSN-Dox (MSN-Dox@GO). After GO wrapping, the TEM image shown in **Fig. 1b** exhibit clear evidence for the complete wrapping of GO sheets around the surface of Dox-loaded MSNs (see high-resolution TEM image in the insets of **Fig. 1a** and **b**). The average hydrodynamic size increased from 76 to 111 nm after GO wrapping (**Fig. 1c**). Zeta potential for MSN-Dox@GO decreased from 12 to -15 mV with increasing mass ratios of GO/MSN from 0.05 to 1 (**Fig. 1d**). When the mass ratio of GO/MSNs was 0.5, zeta potentials of MSNs, GO, MSN-Dox, and GO-MSN-Dox were 18.34, -14.9, 23.56, and -11.7 mV, respectively (**Fig. 1e**).The MSN-Dox@GO kept good stability (**Fig. S2** and **S3**). In addition, the changes in the UV/Vis absorption spectra of GO, MSN and GO-MSN also demonstrated the successful wrapping of GO onto MSNs (**Fig. 1f**). The Dox fluorescence was dramatically quenched after being loaded by MSNs due to self-aggregation of hydrophobic Dox molecules and GO coating (**Fig. S4**).

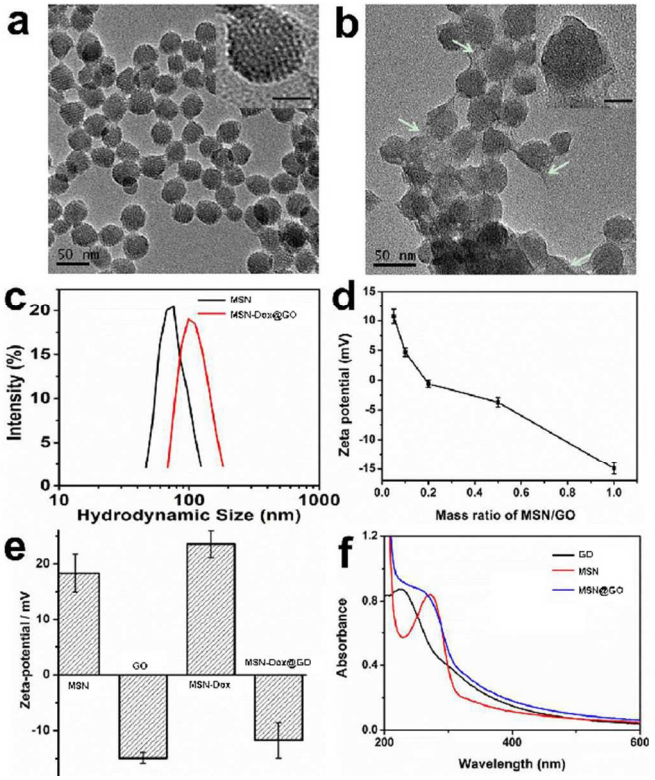

Fig. 1 TEM images of (a) MSN-NH_2, (b) GO-wrapped Dox-loaded MSN (MSN-Dox@GO). The insets scale bar = 20 nm. The white arrows indicate GO sheets, (c) The size distribution of MSN-NH_2 and MSN-Dox@GO, (d) ζ potential changes for MSN-Dox@GO with various mass ratios of GO/MSN. (e) ζ potentials for MSNs, GO sheets, MSN-Dox, and MSN-Dox@GO at GO/MSN mass ratio of 0.5), (f) UV/Vis absorption spectra of GO, MSN and MSN@GO in distilled H_2O.

The *in vitro* drug release profiles of MSN-Dox@GO and MSN-Dox with and without laser irradiation were investigated in pH 7.4 buffer. The temperature change was monitored by an infrared camera. When the MSN-Dox@GO solution was irradiated by a 808 nm laser (0.25 W/cm^2) for six on/off cycles, the change in temperature was consistent, exhibiting a 8~10 ºC increase at each laser irradiation (**Fig. 2a**). **Fig. 2b** shows the slow release of MSN-Dox without and with laser irradiation, which corroborates with the slow drug release profile of typical Dox loaded MSNs. No

significant difference in release amount of Dox with and without laser is attributed to the weak temperature increase of MSN-Dox solution with laser (**Fig. S5**). To achieve a NIR light-triggered drug release, 808 nm NIR laser at 0.25 W/cm^2 was used to irradiate the MSN-Dox@GO solution, which raised the temperature by 34 °C. As the GO gatekeeper converted NIR light into heat, resulting in the high local temperature as well as the expansion of GO sheets and the vibration of GO and MSNs, consequently fast release of Dox. TEM images of MSN-Dox@GO after laser irradiation showed the detachment of GO sheets from MSNs (**Fig. S6**). Since light can be operated very conveniently and precisely, the MSN@GO is an ideal carrier to deliver drugs in a light-responsive mechanism with exact control of the area, time, and dosage of laser irradiation.

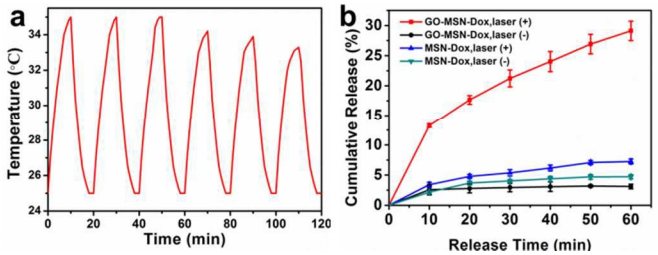

Fig. 2 (a) Temperature plot of MSN-Dox@GO solution irradiated by an 808 nm laser (0.25 W/cm^2) for six on/off cycles (on: 10 min, off: 10 min). (b) Dox release profiles of MSN-Dox@GO and MSN-Dox with and without NIR laser irradiation.

Targeted delivery is one critical demand of nanomedicine.[32-34] Cy5.5-labeled AS1411 aptamer was used as targeting ligand to functionalize the surface of GO. After incubation of Cy5.5-AS1411 and MSN-Dox@GO for 15 min, nearly 80% of the fluorescence was quenched (**Fig. S7**) because of fluorescence resonance energy transfer between Cy5.5 and GO, which implies successful non-covalent assembly of Cy5.5-AS1411 on the surface of GO. The fluorescence response of Cy5.5 towards the target nucleolin (NCL) was tested against different concentrations of NCL ranging from 0.05 to 0.25 μM. No obvious fluorescence change was observed within several aging days (**Fig. S8**), which indicates that Cy5.5-AS1411 kept stable assembly on surface of MSN-Dox@GO, and do not dissociate from the GO sheets in nature. In **Fig. 3**, a significant increase of fluorescence was observed with the increase of NCL concentration. In contrast, negligible amount of fluorescence were recovered when incubated with bovine serum albumin (BSA), which demonstrated high NCL binding affinity and specificity of MSN-Dox@GO-Apt.

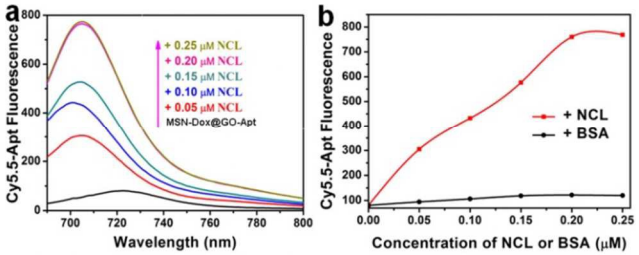

Fig. 3 The fluorescence response of MSN-Dox@GO-Apt towards nucleolin (NCL). (a) Fluorescence emission spectra of 0.05 μM Cy5.5-Apt quenched with GO (black line) and fluorescence recovery by adding NCL with concentration range of 0.05~0.25 μM (from bottom to top). (b) The fluorescence intensity of Cy5.5-Apt with the addition of NCL and BSA.

After the exposure of MSN-Dox@GO-Apt to NCL positive MCF-7 cancer cells, it selectively bound to the surface of cells with high NCL expression, and then triggered receptor-mediated endocytosis. Once the selective targeting was achieved, the Cy5.5 fluorescence was recovered. This reported the endocytosis process of MSN-Dox@GO-Apt, and suggested a suitable time to start laser irradiation. NCL specificity of MSN-Dox@GO-Apt was confirmed by effective blocking of Cy5.5 signal when MCF-7 cells were incubated with MSN-Dox@GO-Apt and free AS1411 (**Fig. S9**).

In the control experiment, 293T cells with low expression of NCL, no Cy5.5 fluorescence was observed regardless of incubation time (**Fig. S10**). With the indication of the recovery of Cy5.5 fluorescence in MCF-7 cells, NIR light triggered Dox release was investigated. After incubation for 4 h, MCF-7 cells were irradiated with 808 nm laser for 10 min, and then further incubated for 2 h. As shown in **Fig. 4**, the Cy5.5 fluorescence was observed inside the cytoplasm and Dox was released into the nucleus upon laser irradiation, whilst no release of Dox was observed without the presence of laser irradiation.

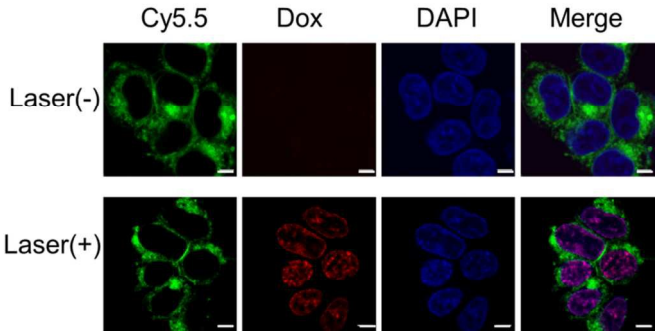

Fig. 4 The fluorescence of MCF-7 cells incubated with MSN-Dox@GO-Apt (Dox equivalent concentration is 0.2 μg/mL) for 4 h (a) without and (b) with laser (808 nm, 0.25 W/cm^2) for 10 min. Dox (red color), Cy5.5-Apt (green color) and nucleus stained with DAPI (blue color) were recorded. Scale bar is 5 μm.

The cytotoxicity of MSN-Dox@GO-Apt, MSN-Dox@GO, MSN-Dox and free Dox to MCF-7 cells was studied by MTT assay. All four formulas exhibited dose-dependent cytotoxicity (**Fig. 5a**). MSN-Dox@GO-Apt and MSN-Dox@GO exhibited less cytotoxicity than free Dox and MSN-Dox, suggesting that only very little amount of Dox was released from MSN-Dox@GO-Apt and MSN-Dox@GO in MCF-7 cells without laser irradiation. The chemotherapeutic efficacy of MSN-Dox@GO-Apt in MCF-7 cells was also evaluated in the presence of laser. A low power density laser of 0.25 W/cm2 was chosen to avoid killing MCF-7 cells directly by the hyperthermic effect of GO (**Fig. 5b**). Because the hyperthermic effect is related to GO, the cells treated with MSN@GO-Apt for 4 h and then irradiated by laser for 10 min were used as a control. No obvious decrease in viability was observed after laser irradiation, which indicates that the hyperthermic effect of MSN@GO-Apt itself does not kill cells. When MCF-7 cells were incubated with MSN-Dox@GO-Apt, a significant dose-dependent cell death was observed after laser irradiation, in accordance with the results from live/dead cell staining (**Fig. 5c**). We studied the cell cytotoxicity of GO on human breast cancer MCF-7 cells, which indicated GO exhibited

negligible toxicity to MCF-7 cells at all of the studied concentrations (1~10 μg/mL) by MTT assay (**Fig. S11**). There will not worry about the cytotoxicity induced by the dissociation of GO from the MSNs nanoparticles. The above results demonstrate that the increased cell death and loss of cell viability was caused by laser-triggered Dox release, thus inducing chemotherapy.

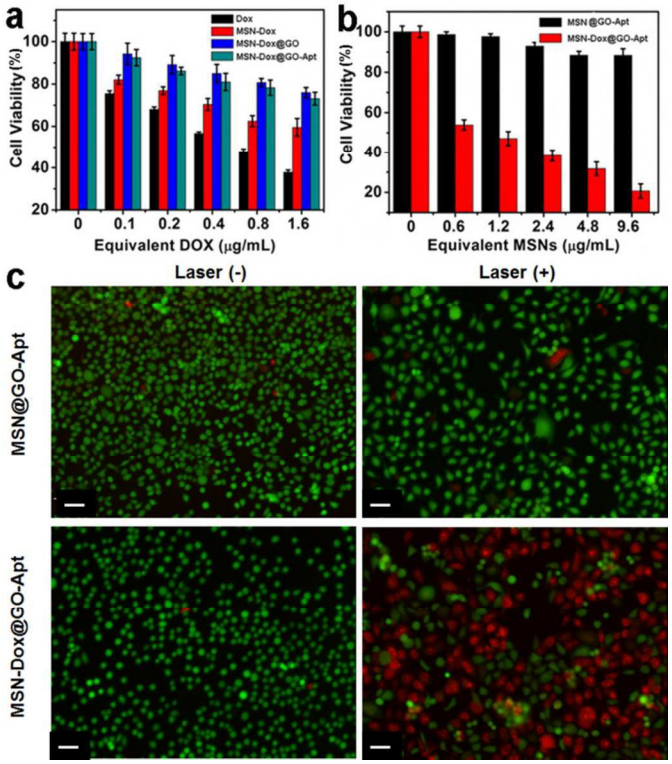

Fig. 5 *In vitro* viability of MCF-7 cells incubated with (a) free DOX, MSN-DOX, MSN@GO-Apt and MSN-Dox@GO-Apt for 24 h, (b) MSN@GO-Apt and MSN-Dox@GO-Apt with laser irradiation for 10 min, (c) Fluorescence images of MCF-7 cells treated with MSN@GO-Apt and MSN-Dox@GO-Apt at 2.4 μg/mL MSNs equivalent concentration for 4 h and then irradiated with laser for 10 min and incubated for further 24 h. Calcein (green, live cells) and PI (red, dead cells). The laser wavelength is 808 nm and power density is 0.25 W/cm^2. Scar bar is 10 μm.

The synergistic dual-mode chemotherapy and photothermal therapy (PTT) of MSN-Dox@GO-Apt were further investigated on MCF-7 cells (**Fig. 6**). At low power density (0.25 W/cm^2) laser irradiation, 57.0% of cells were killed by chemotherapy, and only 1.86% of cells were killed by PTT. At higher power density (0.5 W/cm^2) laser irradiation, 25.6% of cells were killed by chemotherapy, and 43.1% of cells were killed by PTT (**Fig. 6a** and **b**). With the increase of laser power, the main therapeutic effect shifted from chemotherapy to PTT. The similar results were also evidenced by live/dead cell staining (**Fig. 6c**). These results indicate that synergistic therapies of chemotherapy and PTT exhibit much higher therapeutic efficacy compared to either individual chemotherapy or PTT alone.

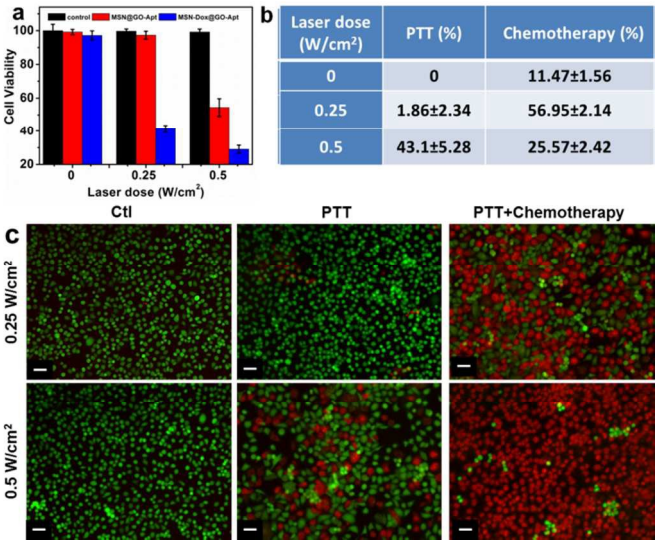

Fig. 6 (a) NIR light triggered synergistic therapies of MSN-Dox@GO-Apt at different laser power densities. (b) PTT and therapy percentages of MSN-Dox@GO-Apt at different laser power densities. (c) Fluorescent imaging of MCF-7 cells treated with MSN@GO-Apt or MSN-Dox@GO-Apt at 2.4 μg/mL MSNs equivalent concentration for 4 h and then irradiated with laser for 10 min and stained with Live/Dead assay after further incubation for 24 h, cells only irradiated with laser were control. Calcein (green, live cells) and PI (red, dead cells). The wavelength of laser is 808 nm and power density is 0.25 and 0.5 W/cm^2. Scar bar is 10 μm.

Experimental Section

Materials: Millipore water (18 MΩ cm; Millipore Co., USA) was used in all experiments. Nucleolin peptide was purchased from Abcam (ab25315). AS1411 aptamer with Cy5.5 modification at the 5'- end (sequence: 5'-Cy5.5-TTG GTG GTG GTG GTT GTG GTG GTG GTG G-3') was purchased from IDT DNA, Inc. with HPLC-purify. Live/dead stain kit was purchased from Invitrogen (Grand Island, NY). Cetyltrimethylammonium bromide (CTAB), 3-aminopropyltrimethoxysilane (APTES, >99%), tetraethylorthosilicate (TEOS), anhydrous ethanol and ammonia (NH_3•H_2O) were purchased from Sigma-Aldrich Chemical Co. and used as received without further purification.

Instruments: Transmission electron microscope (TEM) images were recorded using a Tecnai TF30 TEM (FEI, Hillsboro, OR) equipped with a Gatan Ultrascan 1000 CCD camera (Gatan, Pleasaton, CA) at an accelerating voltage of 120 kV. UV-Vis spectra were acquired on a Genesys 10S spectrophotometer (Thermo Scientific, Waltham, MA) with a 1 cm path length quartz cell. Fluorescence measurements were recorded on an F-7000 fluorescence spectrophotometer (Hitachi, Tokyo, Japan). Zeta potential and particle size were performed using by a SZ-100 nano particle analyzer (HORIBA Scientific, USA). Cell fluorescence images were observed by an IX81 Epifluorescence microscope (Olympus, Hamburg, Germany).

Synthesis of MSNs-NH_2

APTES modified MSNs were fabricated according to the reported method.[35-37] Briefly, 0.29 g of CTAB was dissolved in 150 mL of

0.256 M $NH_3 \cdot H_2O$ solution at 50 °C. After one hour, 2.5 mL of 0.88 M TEOS ethanol solution was added under vigorously stirring. After 15 min, 0.5 mL of APTES was added into the solution. The system was aged for another 20 h. Then the as-synthesized MSNs were centrifuged at 14000 rpm for 30 min and washed for five times with water and ethanol alternatively. The nanoparticles were then transferred to 50 mL of acidic ethanol solution (1 mL of HCl/1L of ethanol) and heated to 60 °C for two hours under stirring. The extracted nanoparticles were further washed three times with ethanol and re-dispersed in water for further use.

Synthesis of MSN-Dox@GO-Apt

Typically, 5 mg of MSNs was mixed with 10 mL of 0.25 mg/mL Dox phosphate-buffered saline (PBS) solution at pH 7.4. The mixture was stirred for 24 h under dark condition. Then Dox loaded MSNs (MSN-Dox) was collected by centrifugation at 14000rpm for 10 min and washed for several times to remove unloaded Dox. For GO wrapping, MSN-Dox was mixed with GO under sonication for several minutes and then stirred for 24 h to get GO wrapped MSN-Dox (MSN-Dox@GO).

Dox loading efficiency

To evaluate the Dox-loading efficiency, the supernatant and washed solutions were measured by using UV-Vis spectrometer at a wavelength of 490 nm to calculate the free Dox content.

***In vitro* release experiment**

For *in vitro* release experiments, MSN-Dox@GO (equivalent of MSNs is 1 mg) was suspended in 1 mL PBS and irradiated with 808 nm laser for 10 min and then centrifuged at 14000 rpm for 10 min to obtain the supernatant and added 1 mL fresh PBS to sediment. The laser spot was adjusted to cover the whole surface of the samples. This procedure repeated for 6 times. During the laser irradiation, the real-time thermal imaging was recorded by a SC300 infrared thermal camera (FLIR, Arlington, VA) and the temperature of whole solution was quantified by FLIR Examiner software. Other control groups were operated with the same condition except irradiation. The released Dox was quantified by UV-Vis spectrophotometer.

***In vitro* fluorescence recovery of Cy5.5 on MSN-Dox@GO-Apt complex**

To investigate the fluorescence recovery of Cy5.5, we added nucleolin peptide, the target of AS1411 aptamer, into the MSN-Dox@GO-Apt complex. BSA was used as control. Fluorescence spectra were recorded on an F-7000 fluorescence spectrophotometer (Hitachi, Tokyo, Japan).

Cytotoxicity assays

MTT assays were used to measure cellular viability. Human breast cancer MCF-7 cells were seeded at a density of 5000 cells/well in 96-well plates for 24 h, and then incubated with free Dox, MSN-Dox MSN-Dox@GO or MSN-Dox@GO-Apt (The equivalent Dox concentrations are 0.1, 0.2, 0.4, 0.8 and 1.6 μg/mL, respectively) for another 24 h. The standard MTT assay was carried out to evaluate the cell viability. Five replicates were done for each group.

***In vitro* aptamer-targeting fluorescence imaging**

For aptamer-targeting imaging, 10^5 of MCF-7 cells/well were seeded in 24-well assay plates. MSN-Dox@GO-Apt (The equivalent aptamer concentration is 0.2 μM) was added and incubated for 1, 2, and 4 h. The cells were then washed for three times with PBS. 500 μL of fixing solution (1% glutaraldehyde and 10% formaldehyde) was added to each well and incubated for 30 min. Finally, the fluorescence images were recorded using an Olympus BX-51 optical system microscopy. Pictures were taken with an Olympus digital camera.293T cells were studied as the same procedure as control.

NIR light triggered Dox release and therapy efficacy

To investigate therapeutic effects of NIR light triggered drug release on MCF-7 cells, 5000 cells/well were seeded in 96-well plate and incubated for 24 h. Then the cells were exposed to MSN-Dox@GO-Apt or MSN@GO-Apt at different MSNs equivalent concentrations for 4 h. Then cells were irradiated by 808 nm laser with a power density of 0.25W/cm^2 for 10 min and incubated for further 24 h. The standard MTT assay was carried out to evaluate the cell viability. 2×10^4 of MCF-7 cells/well were seeded in 12-well plate for 24 h and incubated with MSN-Dox@GO-Apt or MSN@GO-Apt at 2.4 μg/mL MSNs equivalent concentration for 4 h. Then cells were irradiated by 808 nm laser with a power density of 0.25W/cm^2 for 10 min and changed the medium into fresh one and cells were incubated for further 24 h, and stained with live/dead stain kit.

NIR light triggered synergistic therapies of chemotherapy and photothermal therapy

MCF-7 cells were seeded in 96-well plates at a density of 5000 cells per well for 24 h. Then cells were incubated with MSN@GO-Apt or MSN-Dox@GO-Apt solution at 2.4 μg/mL MSN equivalent concentration for 4 h. Afterwards, the cells were irradiated with an 808 nm laser at 0.25 and 0.5 W/cm^2 for 10 min, respectively. After laser irradiation, cells were incubated at 37 °C for further 24 h. Cell viability was measured by MTT assay and live/dead assay. The only laser irradiation group was used as control.

Conclusions

In summary, we have developed a novel aptamer-targeted photoresponsive drug delivery system with two "off-on" switches, based on non-covalent assembling of Cy5.5-AS1411 on the surface of graphene oxide wrapped Dox-loaded mesoporous silica nanoparticles (MSN-Dox@GO-Apt), for light-mediated drug release and aptamer-targeted cancer therapy. The first "off-on" switch was achieved by Cy5.5-AS1411 ligand directed specific targeting of breast cancer MCF-7 cell, thus leading to Cy5.5 fluorescence recovery as a real-time indicator of the endocytosis process of MSN-Dox@GO-Apt. The second "off-on" switch was conducted by laser irradiation. GO transduces NIR light into heat and the local high temperature leads to the expansion of GO sheets and vibration of GO and MSNs, causing on-demand Dox release. This novel "off-on" PDDS system is very promising for targeted drug delivery, controllable drug release and synergistic dual-mode therapies of chemotherapy and PTT.

Acknowledgements

This work was supported in part, by the National Key Basic Research Program of the PRC (2014CB744504, 2014CB744503, 2013CB733802 and 2011CB707700), the Major International (Regional) Joint Research Program of China (81120108013), the National Natural Science Foundation of China (81201175, 81371611, 81371596, 81401465), the China Postdoctoral Science Foundation (2014T71012 and 2013M542576) and Jiangsu planned Projects for Postdoctoral

Research Funds (1301023) and by the Intramural Research Program (IRP) of the NIBIB, NIH.

Notes

[a] *Department of Medical Imaging, Jinling Hospital, School of Medicine, Nanjing University, Nanjing 210002, P.R. China*

[b] *Laboratory of Molecular Imaging and Nanomedicine (LOMIN), National Institute of Biomedical Imaging and Bioengineering (NIBIB), National Institutes of Health, Bethesda, Maryland 20892, United States*

[c] *State Key Laboratory of Molecular Vaccinology and Molecular Diagnostics, Center for Molecular Imaging and Translational Medicine, School of Public Health, Xiamen University, Xiamen, P.R. China*

Reference

1 S. Swaminathan, J. Garcia-Amoros, A. Fraix, N. Kandoth, S. Sortino and F. M. Raymo, *Chem. Soc. Rev.,* 2014, **43**, 4167-4178.
2 S. Mura, J. Nicolas and P. Couvreur, *Nat. Mater.,* 2013, **12**, 991-1003.
3 E. Fleige, M. A. Quadir and R. Haag, *Adv. Drug Deliv. Rev.,* 2012, **64**, 866-84.
4 D. He, X. He, K. Wang, Z. Zou, X. Yang and X. Li, *Langmuir*, 2014, **30**, 7182-7189.
5 P. Rai, S. Mallidi, X. Zheng, R. Rahmanzadeh, Y. Mir, S. Elrington, A. Khurshid and T. Hasan, *Adv. Drug Deliv. Rev.,* 2010, **62**, 1094-1124.
6 P. Huang, P. Rong, J. Lin, W. Li, X. Yan, M. G. Zhang, L. Nie, G. Niu, J. Lu, W. Wang and X. Chen, *J. Am. Chem. Soc.,* 2014, **136**, 8307-8313.
7 P. Huang, J. Lin, X. Wang, Z. Wang, C. Zhang, M. He, K. Wang, F. Chen, Z. Li, G. Shen, D. Cui and X. Chen, *Adv. Mater.,* 2012, **24**, 5104-5110.
8 P. Huang, J. Lin, W. Li, P. Rong, Z. Wang, S. Wang, X. Wang, X. Sun, M. Aronova, G. Niu, R. D. Leapman, Z. Nie and X. Chen, *Angew. Chem. Int. Ed. Engl.,* 2013, **52**, 13958-13964.
9 B. P. Timko and D. S. Kohane, *Expert Opin. Drug Deliv.,* 2014, **11**, 1681-1685.
10 C. Coll, A. Bernardos, R. Martinez-Manez and F. Sancenon, *Acc. Chem. Res.,* 2013, **46**, 339-349.
11 Z. Zhang, L. Wang, J. Wang, X. Jiang, X. Li, Z. Hu, Y. Ji, X. Wu and C. Chen, *Adv. Mater.,* 2012, **24**, 1418-1423.
12 J. Lu, E. Choi, F. Tamanoi and J. I. Zink, *Small,* 2008, **4**, 421-426.
13 Q. Yuan, Y. Zhang, T. Chen, D. Lu, Z. Zhao, X. Zhang, Z. Li, C. H. Yan and W. Tan, *Acs Nano,* 2012, **6**, 6337-6344.
14 H. Yan, C. Teh, S. Sreejith, L. Zhu, A. Kwok, W. Fang, X. Ma, K. T. Nguyen, V. Korzh and Y. Zhao, *Angew. Chem. Int. Ed. Engl.,* 2012, **51**, 8373-8377.
15 R. Tong, H. D. Hemmati, R. Langer and D. S. Kohane, *J. Am. Chem. Soc.,* 2012, **134**, 8848-8855.
16 D. He, X. He, K. Wang, J. Cao and Y. Zhao, *Langmuir,* 2012, **28**, 4003-4008.
17 P. Huang, C. Xu, J. Lin, C. Wang, X. Wang, C. Zhang, X. Zhou, S. Guo and D. Cui, *Theranostics,* 2011, **1**, 240-250.
18 K. Yang, L. Feng, X. Shi and Z. Liu, *Chem. Soc. Rev.,* 2013, **42**, 530-547.
19 Z. Sun, P. Huang, G. Tong, J. Lin, A. Jin, P. Rong, L. Zhu, L. Nie, G. Niu and F. Cao, *Nanoscale,* 2013, **5**, 6857-6866.
20 R. M. Kong, X. B. Zhang, Z. Chen and W. Tan, *Small,* 2011, **7**, 2428-2436.
21 M. Yi, S. Yang, Z. Peng, C. Liu, J. Li, W. Zhong, R. Yang and W. Tan, *Anal. Chem.,* 2014, **86**, 3548-3554.
22 Y. Wang, Z. Li, D. Hu, C.-T. Lin, J. Li and Y. Lin, *J. Am. Chem. Soc.,* 2010, **132**, 9274-9276.
23 S. Sreejith, X. Ma and Y. Zhao, *J. Am. Chem. Soc.,* 2012, **134**, 17346-17349.
24 D.-K. Lim, A. Barhoumi, R. G. Wylie, G. Reznor, R. S. Langer and D. S. Kohane, *Nano Lett.,* 2013, **13**, 4075-4079.
25 C. Xu, D. Yang, L. Mei, B. Lu, L. Chen, Q. Li, H. Zhu and T. Wang, *ACS Appl. Mater. Interfaces,* 2013, **5**, 2715-2724.
26 W. Tan, M. J. Donovan and J. Jiang, *Chem. Rev.,* 2013, **113**, 2842-2862.
27 S. Soundararajan, W. Chen, E. K. Spicer, N. Courtenay-Luck and D. J. Fernandes, *Cancer Res.,* 2008, **68**, 2358-2365.
28 J. Guo, X. Gao, L. Su, H. Xia, G. Gu, Z. Pang, X. Jiang, L. Yao, J. Chen and H. Chen, *Biomaterials,* 2011, **32**, 8010-8020.
29 J. Ai, Y. Xu, B. Lou, D. Li and E. Wang, *Talanta,* 2014, **118**, 54-60.
30 J. F. Lovell, C. S. Jin, E. Huynh, H. Jin, C. Kim, J. L. Rubinstein, W. C. Chan, W. Cao, L. V. Wang and G. Zheng, *Nat. Mater.,* 2011, **10**, 324-332.
31 Y. Tang, Y. Liu, Z. Teng, Y. Tian, J. Sun, S. Wang, C. Wang, J. Wang and G. Lu, *J. Mater. Chem. B,* 2014, **2**, 4356-4362.
32 Z. Li, P. Huang, X. Zhang, J. Lin, S. Yang, B. Liu, F. Gao, P. Xi, Q. Ren and D. Cui, *Mol. Pharm.,* 2009, **7**, 94-104.
33 P. Huang, L. Bao, C. Zhang, J. Lin, T. Luo, D. Yang, M. He, Z. Li, G. Gao, B. Gao, F. Shen and D. Cui, *Biomaterials,* 2011, **32**, 9796-9809.
34 P. Huang, S. Wang, X. Wang, G. Shen, J. Lin, Z. Wang, S. Guo, D. Cui, M. Yang and X. Chen, *J. Biomed. Nanotechnol.,* 2015, **11**, 117-125.
35 Y. S. Lin, N. Abadeer, K. R. Hurley and C. L. Haynes, *J. Am. Chem. Soc.,* 2011, **133**, 20444-20457.
36 Y. S. Lin, N. Abadeer and C. L. Haynes, *Chem. Commun.,* 2011, **47**, 532-534.
37 Y. S. Lin and C. L. Haynes, *J. Am. Chem. Soc.,* 2010, **132**, 4834-4842.

